Polygenic adaptation from standing genetic variation allows rapid ecotype formation

Nico Fuhrmann, Celine Prakash, Tobias S. Kaiser*

Max Planck Institute for Evolutionary Biology,
Max Planck Research Group *Biological Clocks*,
August-Thienemann-Strasse 2, 24306 Plön, Germany

*kaiser@evolbio.mpg.de

Abstract

Adaptive ecotype formation is the first step to speciation, but the genetic underpinnings of this process are poorly understood. Marine midges of the genus *Clunio* (Diptera) have recolonized Northern European shore areas after the last glaciation. In response to local tide conditions they have formed different ecotypes with respect to timing of adult emergence, oviposition behavior and larval habitat. Genomic analysis confirms the recent establishment of these ecotypes, reflected in massive haplotype sharing between ecotypes, irrespective of whether there is ongoing gene flow or geographic isolation. QTL mapping and genome screens reveal patterns of polygenic adaptation from standing genetic variation. Ecotype-associated loci prominently include circadian clock genes, as well as genes affecting sensory perception and nervous system development, hinting to a central role of these processes in ecotype formation. Our data show that adaptive ecotype formation can occur rapidly, with ongoing gene flow and largely based on a re-assortment of existing alleles.

Keywords: Local adaptation, reproductive timing, lunar rhythm, biological clocks, gene flow, Chironomidae, marine ecology

Introduction

The genetic foundations for rapid ecological adaptation and speciation remain poorly understood. Decades of research have focused on identifying single or few major genetic loci in such contexts, with some notable successes [1-4]. However, many genome-wide association studies have now shown that quantitative trait phenotypes have usually a polygenic basis[5,6]. This implies that also rapid natural adaptation should be expected to occur in a polygenic context[7,8]. Yet, tests of this assumption are still rare, since it is easier to prove the involvement of major locus compared to showing its absence. To show that this occurs in natural populations requires an exceptional biogeographic setting, as well as deep genomic and genetic analysis.

Here we present a study on the postglacial evolution of new ecotypes in marine midges of the genus *Clunio* (Diptera: Chironomidae), which in adaptation to their habitat differ in oviposition behavior and reproductive timing, involving both circadian and circalunar clocks.

Circalunar clocks are biological time-keeping mechanisms that allow organisms to anticipate lunar phase[9]. Their molecular basis is unknown[10], making identification of adaptive loci for lunar timing both particularly challenging and interesting. In many marine organisms, circalunar clocks synchronize reproduction within a population. In *Clunio marinus* they have additional ecological relevance[11]. Living in the intertidal zone of the European Atlantic coasts, *C. marinus* requires the habitat to be exposed by the tide for successful oviposition. The habitat is maximally exposed during the low waters of spring tide days around full moon and new moon. Adult emergence is restricted to these occasions by a circalunar clock, which tightly regulates development and maturation. Additionally, a circadian clock ensures emergence during only one of the two daily low tides. The adults reproduce immediately after emergence and die few hours later. As tidal regimes vary dramatically along the coastline, populations of this *Atlantic ecotype* of *C. marinus* show local timing adaptations[11-13] for which the genetic underpinnings are partially known[14,15].

When *Clunio* expanded into the North after the recess of the ice shield, new ecotypes *evolved* in the Baltic Sea[16-18] and in the high Arctic[19,20], which differ from the *Atlantic ecotype* of *C. marinus* in various ways (see Fig. 1 for a summary of defining characteristics of the three ecotypes). In the Baltic Sea the tides are negligible and the *Baltic ecotype* oviposits on the

open water, from where the eggs quickly sink to the submerged larval habitat at water depths of up to 20 metres[16,21]. Reproduction of the *Baltic ecotype* happens every day precisely at dusk under control of a circadian clock[22], without a detectable circalunar rhythm[17]. Near Bergen (Norway) the *Baltic* and *Atlantic ecotypes* were reported to co-occur in sympatry, but in temporal reproductive isolation. The *Baltic ecotype* reproduces at dusk, the *Atlantic ecotype* reproduces during the afternoon low tide[22]. Therefore, the *Baltic ecotype* is currently considered a separate species – *C. balticus*. However, *C. balticus* and *C. marinus* can be successfully interbred in the laboratory[22].

In the high Arctic there are normal tides and the *Arctic ecotype* of *C. marinus* is found in intertidal habitats[19]. During its reproductive season, the permanent light of polar day precludes synchronization of the circadian and circalunar clocks with the environment. Thus, the *Arctic ecotype* relies on a so-called tidal hourglass timer, which allows it to emerge and reproduce during every low tide[20]. It does not show circalunar or circadian rhythms[20].

The geological history of Northern Europe[23] implies the Baltic Sea and the high Arctic could only be colonized by *Clunio* after the last glacial ice shield recessed about 10,000 years ago. This inference is also supported by subfossil *Clunio* head capsules in Baltic Sea sediment cores[24]. The new adaptations to the absence of tides in the Baltic Sea and to polar day in the high Arctic must therefore have occurred within this time frame. This makes *Clunio* a particularly interesting model system for studying the genetics of rapid adaptation, since it promises at the time to yield insights into the genetic pathways underlying the ecotype characteristics, including circadian and circalunar timing.

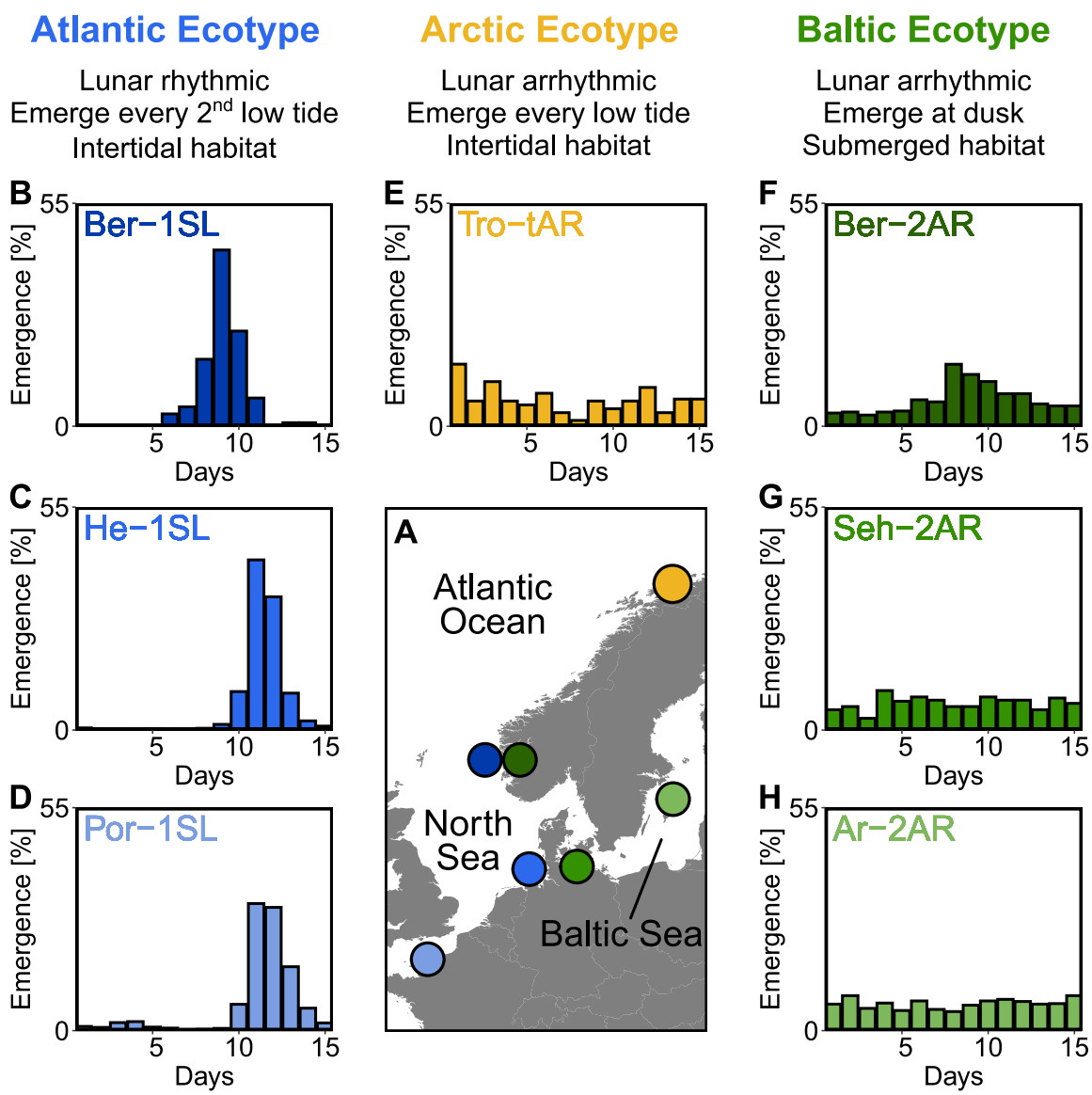

Figure 1 **Northern European ecotypes of *Clunio* and their lunar rhythms**

The *Atlantic*, *Arctic* and *Baltic ecotypes* of *Clunio* differ mainly in their lunar rhythms (B-H), circadian rhythms (Suppl. Fig. 1), as well as their habitat and the resulting oviposition behavior (Suppl. Note 1). **(A)** Sampling sites for this study. **(B-H)** Lunar rhythms of adult emergence in corresponding laboratory strains under common garden conditions, with 16 hours of daylight and simulated tidal turbulence cycles to synchronize the lunar rhythm. In *Arctic* and *Baltic ecotypes* the lunar rhythm is absent (E,G,H) or very weak (F). Por-1SL: n=1,263; He-1SL: n=2,075; Ber-1SL: n=230; Tro-tAR: n=209; Ber-2AR: n=399; Seh-2AR: n= 380; Ar-2AR: n=765.

91 # Results

92

93 ***Clunio* ecotypes.** Starting from field work in Northern Europe (Fig. 1A), we established one
94 laboratory strain of the *Arctic ecotype* from Tromsø (Norway, Tro-tAR; see methods for strain
95 nomenclature) and three laboratory strains of the *Baltic ecotype*, from Bergen (Norway, Ber-
96 2AR), Sehlendorf (Germany; Seh-2AR) and Ar (Sweden; Ar-2AR). We also established a strain
97 of the *Atlantic ecotype* from Bergen (Ber-1SL, sympatric with Ber-2AR) and used two existing
98 *Atlantic ecotype* laboratory strains from Helgoland (Germany; He-1SL) and Port-en-Bessin
99 (France; Por-1SL). We confirmed the identity of the ecotypes in the laboratory by the absence
100 of a lunar rhythm in the *Baltic* and *Arctic ecotypes* (Fig. 1B-H), their circadian rhythm (Supple-
101 mentary Fig. 1B-H) and their oviposition behavior (for details see Supplementary Note 1). The
102 *Baltic ecotype* from Bergen (Ber-2AR, Fig. 1F) was found weakly lunar-rhythmic.

103

104 **Evolutionary history and species status.** We sequenced the full nuclear and mitochondrial
105 genomes of 168 field-caught individuals from six geographic sites, including the two sympatric
106 population ecotypes from Bergen (Figure 1). Based on a set of 792,032 single nucleotide pol-
107 ymorphisms (SNPs), we first investigated population structure and evolutionary history by
108 performing a principal component analysis (PCA; Fig. 2A-B) and testing for genetic admixture
109 (Fig. 2C). We also constructed a haplotype network of complete mitochondrial genomes (Fig.
110 2D). There are several major observations that can be derived from these data.
111 First, there is strong geographic isolation between populations from different sites. In PCA,
112 clusters are formed according to geography (Fig. 2A-B, Supplementary Fig. 2). Mitochondrial
113 haplotypes are not shared and are diagnostically different between geographic sites (Fig. 2D).
114 In ADMIXTURE, the optimal number of genetic groups is six (Fig. 2C, Supplementary Fig. 3),
115 corresponding to the number of geographic sites, and there is basically no mixing between
116 the six clusters (Fig. 2C; K=6). Finally, there is isolation by distance (IBD; Supplementary Figure
117 4).

118 Second, and much in contrast to the above, the sympatric ecotypes in Bergen are genet-
119 ically very similar. In PCA they are not separated in the first four principal components (Fig.
120 2A-B) and they are the only populations that share mitochondrial haplotypes (Fig. 2D). In the

ADMIXTURE analysis, they are only distinguished at K=7, a value larger than the optimal K. As soon as the two populations are distinguished, some individuals show signals of admixed origin (Fig. 2C; K=7), indicative of ongoing gene flow and incomplete reproductive isolation. These observations question the species status of *C. balticus*, which was based on the assumption of temporal isolation between these two populations[22].

Third, the data suggest that after the ice age *Clunio* colonized northern Europe from a single source and expanded along two fronts into the Baltic Sea and into the high Arctic. The mitochondrial haplotype network expands from a single center, which implies a quick radiation from a colonizing haplotype (Fig. 2D; note that all sampled populations occur in areas under a former ice shield cover). There is also a large degree of shared nuclear polymorphisms. 34% of polymorphic SNPs are polymorphic in all seven populations and 93% are polymorphic in at least two populations (Supplementary Fig. 5). Separation of the Baltic Sea populations along PC1 and the Arctic population along PC2 (Fig. 2A), suggests that *Clunio* expanded into the high Arctic and into the Baltic Sea independently. Congruently, nucleotide diversity significantly decreases towards both expansion fronts (Supplementary Fig. 6, Supplementary Tab. 1). Post-glacial establishment from a common source indicates that the *Baltic* and *Arctic ecotypes* have evolved their new local adaptations during this expansion time, i.e., in less than 10,000 years.

Figure 2 Genetic structure and evolutionary history of Northern European *Clunio* ecotypes

The analysis is based on 24 individuals from each population (23 for Por-1SL, 25 for He-1SL). **(A,B)** Principal Component Analysis (PCA) based on 792,032 SNPs separates populations by geographic location rather than ecotype. **(C)** ADMIXTURE analysis supports strong differentiation by geographic site (best K=6), but a notable genetic component from the Baltic Sea in the Bergen populations (see K=2 and 3). The Bergen populations are only separated at K=7 and then show a number of admixed individuals. **(D)** Haplotype network of full mitochondrial genomes reveals highly divergent clusters according to geographic site, but haplotype sharing between Ber-1SL and Ber-2AR. **(E)** Correlated allele frequencies indicate introgression from Seh-2AR into Ber-2AR.

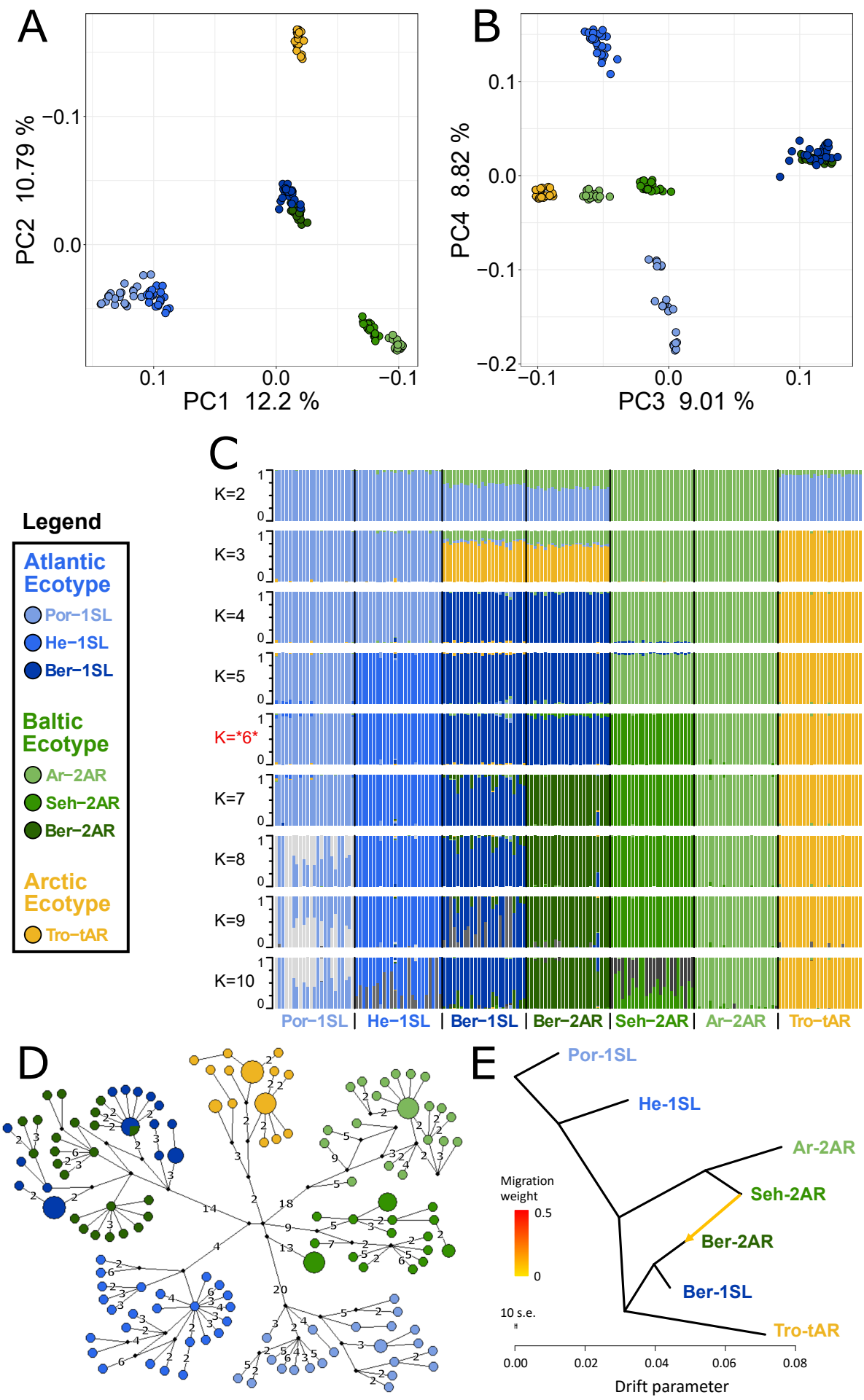
A
PC2 10.79 %
PC1 12.2 %
B
PC4 8.82 %
PC3 9.01 %
C
Legend
Atlantic Ecotype
Por−1SL
He−1SL
Ber−1SL
Baltic Ecotype
Ar−2AR
Seh−2AR
Ber−2AR
Arctic Ecotype
Tro−tAR
K=2
K=3
K=4
K=5
K=*6*
K=7
K=8
K=9
K=10
Por−1SL | He−1SL | Ber−1SL | Ber−2AR | Seh−2AR | Ar−2AR | Tro−tAR
D
E
Por-1SL
He-1SL
Ar-2AR
Seh-2AR
Ber-2AR
Ber-1SL
Tro-tAR
Migration weight
0.5
0
10 s.e.
0.00
0.02
0.04
0.06
0.08
Drift parameter

154 Fourth, ADMIXTURE analysis reveals that sympatric co-existence of the *Atlantic* and *Baltic*
155 *ecotypes* in Bergen likely results from introgression of *Baltic ecotype* individuals into an exist-
156 ing *Atlantic ecotype* population. At K=2 and K=3 the two Baltic Sea populations Seh-2AR and
157 Ar-2AR are separated from all other populations and the two Bergen populations Ber-2AR and
158 Ber-1SL show a marked genetic contribution coming from these Baltic Sea populations (Fig.
159 2C). The Baltic genetic component is slightly larger for the *Baltic ecotype* Ber-2AR population
160 than for the *Atlantic ecotype* Ber-1SL population. A statistical analysis via TreeMix detects pre-
161 dominantly an introgression from Seh-2AR into Ber-2AR (Fig. 2E, Supplementary Fig. 7), sug-
162 gesting that genetic haplotypes that convey the *Baltic ecotype* have introgressed into a popu-
163 lation of *Atlantic ecotype*, resulting in the now observed sympatric co-existence of *Baltic* and
164 *Atlantic ecotypes* in Bergen.
165 While this observation adds to the evidence for a role of introgression in adaptation and
166 early speciation processes [25,26], it also constitutes an excellent starting point for mapping loci
167 that could be involved in the respective ecotype adaptations. Under the assumption that fast
168 adaptation and ecotype formation are mostly based on frequency changes in standing varia-
169 tion, one expects that the respective haplotypes should be shared between ecotypes, espe-
170 cially when transferred via introgression. The following analysis is focussed on the *Atlantic* and
171 *Baltic ecotypes*, represented by three populations each.
172
173 **Nuclear haplotype sharing.** First, we reconstructed the genealogical relationship between
174 36 individuals (six from each population) in 50 kb windows (n=1,607) along the genome, fol-
175 lowed by topology weighting. There are 105 possible unrooted tree topologies for six popula-
176 tions, and 46,656 possibilities to pick one individual from each population out of the set of 36.
177 For each window along the genome, we assessed the relative support of each of the 105 pop-
178 ulation tree topologies by all 46,656 combinations of six individuals. We found that tree to-
179 pologies change rapidly along the chromosomes (Fig. 3A; Supplementary Fig. 8; Supplemen-
180 tary Data 1). The tree topology obtained for the entire genome (Supplementary Fig. 9) domi-
181 nates only in few genomic windows (Fig. 3A, black bars “Orig.”), while usually one or several
182 other topologies account for more than 75% of the tree topologies (Fig. 3A, grey bars “Misc.”).

183 Hardly ever do all combinations of six individuals follow a single population tree topology (Fig.
184 3A, stars), which implies that in most genomic windows some individuals do not group with
185 their population. Taken together, this indicates a massive sharing of haplotypes across popu-
186 lations and high levels of incomplete lineage sorting, typical for such radiation situations. In
187 such a highly mixed genomic landscape, it is close to impossible to separate signals of intro-
188 gression from incomplete lineage sorting. Still, we highlighted genomic windows that are con-
189 sistent with the detected introgression from the *Baltic ecotype* into both Bergen populations
190 (Fig. 3A, yellow bars "Intr."; all topologies grouping Por-1SL and He-1SL vs Ber-1SL, Ber-2AR,
191 Seh-2AR and Ar-2AR). Regions consistent with introgression are scattered over the entire ge-
192 nome.
193
194 **Crosses and QTL mapping suggest a polygenic basis to lunar rhythmicity.** As a first attempt
195 to get hold of ecologically relevant loci, we assessed the genetic basis to lunar rhythmicity by
196 crossing the lunar-arrhythmic Ber-2AR strain with the lunar-rhythmic Ber-1SL strain. Interest-
197 ingly, the degree of lunar rhythmicity segregates within and between crossing families (Sup-
198 plementary Fig. 10), suggesting a heterogeneous polygenic basis of lunar arrhythmicity. Ge-
199 netic segregation in the cross implies that the weak rhythm observed in Ber-2AR is due to
200 genetic polymorphism. The Ber-2AR strain seems to carry some lunar-rhythmic alleles, likely
201 due to gene flow from the sympatric *Atlantic ecotype* (see Fig. 1C and results below).
202 For QTL mapping, we then picked a set of F2 families, which all go back to a single parental
203 pair (BsxBa-F2 34; n=272 Supplementary Fig. 10). As a phenotype, we scored the degree of
204 lunar rhythmicity for each individual as the number of days between the individual's emer-
205 gence and day 9 of the artificial turbulence cycle, which is the peak emergence day of the
206 lunar-rhythmic strain (Supplementary Fig. 11). However, QTL analysis with various algorithms
207 did not reveal any significant QTL for lunar rhythmicity (Fig. 4). As a control that in principle
208 we had sufficient power for QTL mapping in this crossing family, we also mapped the sex de-
209 termining locus, which was clearly detectable (Fig. 4). We can conclude that lunar rhythmicity
210 must have a polygenic basis with many loci of small effects.
211

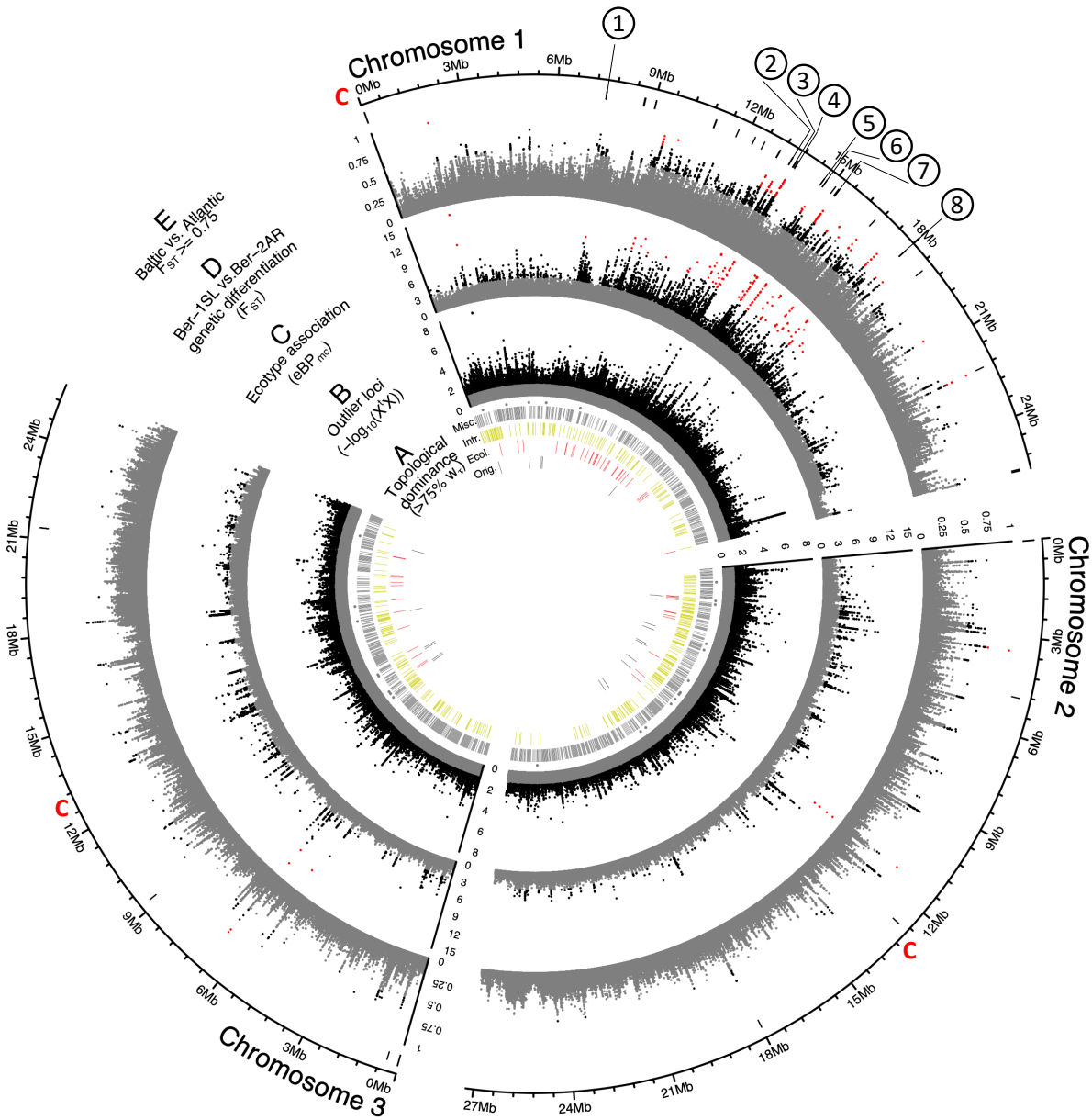

Figure 3 **Genome screens for haplotype sharing and genotype-ecotype associations**

(**A**) Topology weighting of phylogenetic trees for 36 individuals from the *Baltic* and *Atlantic ecotypes*, as obtained from 50 kb non-overlapping genomic windows. Windows were marked by a bar if they were dominated by one kind of topology (w_τ > 75%). Most windows are not dominated by the consensus population topology ("Orig."; Suppl. Fig. 9), but by combinations of other topologies ("Misc."). Windows dominated by topologies that separate the *Baltic* and *Atlantic ecotypes* ("Ecol.") are mostly on chromosome 1. Windows consistent with introgression are found all over the genome ("Intr."). (**B**) Distribution of outlier variants (SNPs and Indels) between the six *Baltic* and *Atlantic ecotype* populations, after global correction for population structure (X^tX statistic). Values below the significance threshold (as obtained by subsampling) are plotted in grey. (**C**) Association of variant frequencies with *Baltic* vs. *Atlantic ecotype* (eBP_{mc}). Values below the threshold of 3 (corresponding to p = 10^{-3}) are given in grey, values above 10 are given in red. (**D**) Genetic differentiation (F_{ST}) between the sympatric ecotypes in Bergen. Values above 0.5 are given in black, values above 0.75 in red. (**E**) The distribution of SNPs with F_{ST} >= 0.75 in the *Baltic* vs. *Atlantic ecotypes*. Circled numbers mark the location of the eight most differentiated loci (see Fig. 6). Centromeres of the chromosomes are marked by a red "C".

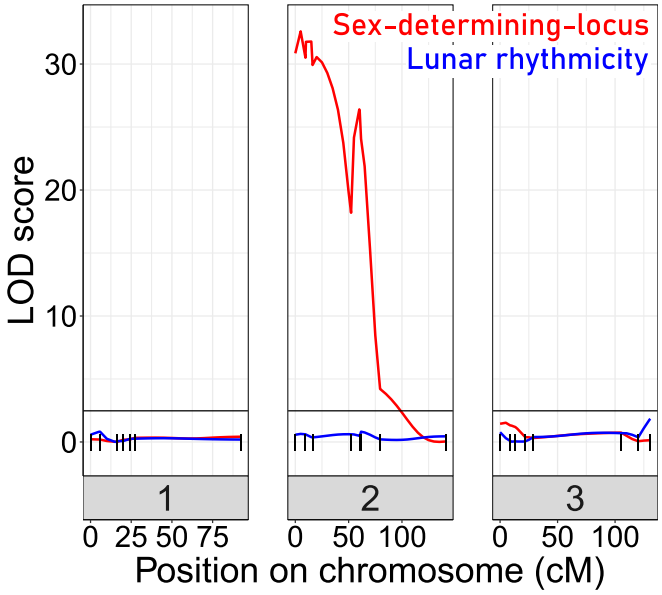

Figure 4 Quantitative Trait Locus (QTL) mapping for lunar rhythmicity and the sex determining locus.

No significant QTLs can be detected for lunar rhythmicity, suggesting it is controlled by many loci of small effects. The sex-determining locus is clearly detectable, indicating that the is no general lack of power in the mapping panel.

Genomic regions associated with ecotype formation. Given that QTL mapping for lunar rhythmicity suggested a polygenic basis to ecotype formation, we next applied three approaches to identify genomic regions associated with divergence between *Atlantic* and *Baltic ecotypes*.

First, genomic windows which are dominated by tree topologies that group populations according to ecotype were highlighted (Fig. 3A, red bars "Ecol.").

Second, we screened all genetic variants (SNPs and indels; n=948,128) for those that are overly differentiated between the six populations after correcting for the neutral covariance structure across population allele frequencies (see Ω matrix, Supplementary Fig. 12A-B). Such variants can indicate local adaptation. At the same time, we tested for association of these variants with ecotype, as implemented in BayPass[27]. Overly differentiated variants (X^tX statistic; Fig. 3B) and ecotype-associated variants ecotype (eBP_{mc}; Fig. 3C) were detected all over the genome, but many were concentrated in the middle of the telocentric chromosome 1. Tests for association of variants with environmental variables such as sea surface temperature or salinity find fewer associated SNPs and no concentration on chromosome 1 (Supplementary Fig. 12D-E), confirming that the detected signals are not due to general genome properties, but are specific to the ecotypes.

257 Third, we expected that gene flow between the sympatric Ber-1SL and Ber-2AR populations
258 would largely homogenize their genomes except for regions involved in ecological adaptation,
259 which would be highlighted as peaks of genetic differentiation. The distributions of F_{ST} values
260 in all pairwise population comparisons confirmed that genetic differentiation was particularly
261 low in the Ber-1SL vs. Ber-2AR comparison (Supplementary Fig. 13 and 14). Pairwise differen-
262 tiation between Ber-1SL and Ber-2AR (Fig. 3D) shows marked peaks on chromosome 1, most
263 of which coincide with peaks in X^tX and eBP_{mc}. Notably, when assessing genetic differentiation
264 of *Baltic* vs *Atlantic ecotype* (72 vs 72 individuals; Fig. 3E; Supplementary Fig. 15), there is not
265 a single diagnostic variant ($F_{ST} = 1$), and even variants with $F_{ST} \geq 0.75$ are very rare (n=63; Fig.
266 3E).
267 Genetic divergence (d_{xy}), nucleotide diversity (π) and local linkage disequilibrium (r^2) of the
268 two Bergen populations do not show marked differences along or between chromosomes
269 (Supplementary Fig. 16). The cluster of ecotype-associated variants on chromosome 1 over-
270 laps with three large blocks of long-range linkage disequilibrium (LD; Supplementary Fig. 17).
271 However, the boundaries of the LD blocks do not correspond to the ecotype-associated region
272 and differ between populations. LD blocks are not ecotype-specific. Local PCA of the strongly
273 ecotype associated region does not reveal patterns consistent with a chromosomal inversion
274 or another segregating structural variant (Supplementary Fig. 18). Thus, there is no obvious
275 link between the clustering of ecotype-associated loci and structural variation. Notably, ge-
276 netic differentiation is not generally elevated in the ecotype-associated cluster on chromo-
277 some 1, as would be expected for a segregating structural variant, but drops to baseline levels
278 in between ecotype-associated loci (Fig. 3D).
279 Taken together, these observations imply that numerous genomic loci – inside and outside
280 the cluster on chromosome 1 – are associated with ecological adaptation and none of these
281 are differentially fixed between ecotypes. In line with QTL mapping, this virtually excludes the
282 possibility that only one or few loci have driven the new ecotype formation, suggesting instead
283 that ecotype formation is based on a complex polygenic architecture.
284

285 **Support for adaptation from standing genetic variation.** If, as assumed above, adaptation
286 in these populations was indeed based mostly on standing genetic variation, one should find
287 evidence in this in the data structure. We selected highly ecotype-associated SNPs (X^tX >
288 1.152094, threshold obtained from randomized subsampling; eBP_{mc} > 3; n=3,976; Supplemen-
289 tary Fig. 19A) and assessed to which degree these alleles are shared between the studied pop-
290 ulations and other populations across Europe. Allele sharing between the Bergen populations
291 is likely due to ongoing gene flow, and hence Bergen populations were excluded from the
292 analysis. In turn, allele sharing between the geographically isolated Seh-2AR, Ar-2AR, Por-1SL
293 and He-1SL populations likely represents shared ancient polymorphism. Based on this com-
294 parison, we found that 82% of the ecotype-associated SNPs are polymorphic in both *Atlantic*
295 and *Baltic ecotypes*, suggesting that the largest part of ecotype-associated alleles originates
296 from standing genetic variation. We then retrieved the same genomic positions from pub-
297 lished population resequencing data for *Atlantic ecotype* populations from Vigo (Spain) and
298 St. Jean-de-Luz (Jean, southern France)[14], an area that is potentially the source of postglacial
299 colonization of all locations in this study. We found that 90% of the alleles associated with the
300 Northern European ecotypes are also segregating in at least one of these southern popula-
301 tions, supporting the notion that adaptation in the North involves a re-assortment of existing
302 standing genetic variation.
303
304 **Ecotypes differ mainly in the circadian clock and nervous system development.** In the light
305 of a polygenic architecture for ecotype formation, we can expect that usually several genes of
306 a relevant physiological pathways are affected. This provides an ideal setting to identify the
307 physiological processes underlying ecotype formation by enrichment analysis. Accordingly, we
308 assessed how all ecotype-associated variants (SNPs and indels; X^tX > 1.148764; eBP_{mc} > 3,
309 n=4,741; Supplementary Fig. 19B) relate to *C. marinus'* genes. In a first step, we filtered the
310 existing gene models in the CLUMA1.0 reference genome to those that are supported by tran-
311 script or protein evidence, have known homologues or PFAM domains, or were manually cu-
312 rated (filtered annotations provided in Supplementary Data 2; 15,193 gene models). Based on
313 this confidence gene set, we then assessed the location of variants relative to genes, as well

314 as the resulting mutational effects (SNPeff[28]; Supplementary Fig. 20; statistics in Supplemen-
315 tary Tab. 2). The vast majority of ecotype-specific variants are classified as intergenic modifier
316 variants, suggesting that ecotype formation might primarily rely on regulatory mutations.

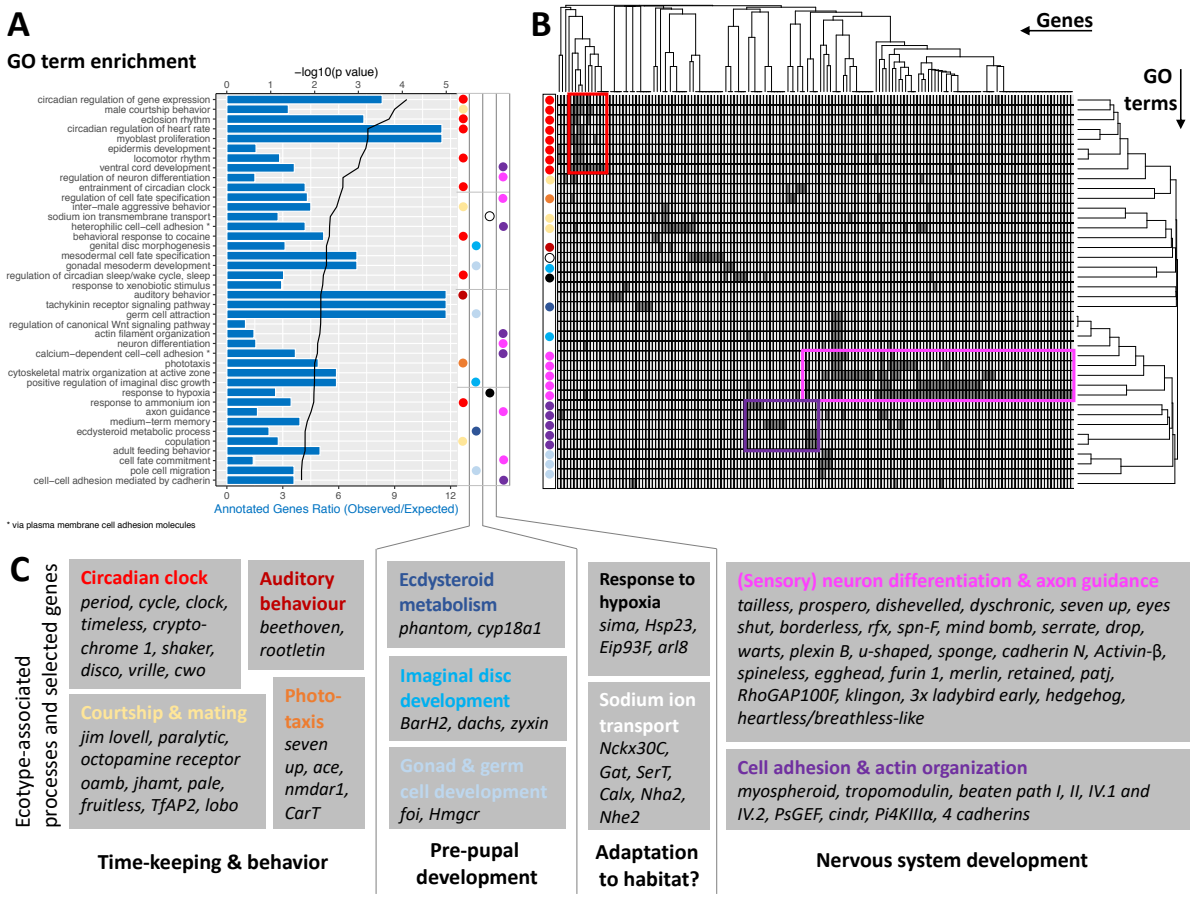

317
318 **Figure 5 GO term analysis of ecotype associated SNPs**
319
320 (**A**) The top 40 enriched GO terms are listed for the 1,400 genes that are found to be affected by eco-
321 type-associated genetic variants ($eBP_{mc} > 3$). For each GO term the significance level (black line, top y-
322 axis) and the observed-expected ratio of genes annotated to the respective GO term (blue bars, bot-
323 tom y-axis) are given. (**B**) The top 40 GO terms are driven by 168 genes. Hierarchical clustering of
324 genes and GO terms reveals major signals in the circadian clock and nervous system development
325 (more details in Supplementary Table 3). (**C**) Most GO terms are consistent with the known ecotype
326 differences and selected genes are highlighted for all of them. Notably, basically all core circadian
327 clock genes are affected.

328 The ecotype-specific SNPs are found in and around 1,400 genes (Supplementary Data 3 and
329 4). We transferred GO terms from other species to the *Clunio* confidence annotations based
330 on gene orthology (5,393 genes; see methods and Supplementary Data 5). GO term enrich-
331 ment analysis suggests that ecological adaptation prominently involves the circadian clock,
332 supported by three of the top four GO terms (Fig. 5A). In order to identify which genes drive
333 GO term enrichment in the top 40 GO terms, we extracted the genes that harbour ecotype-
334 associated SNPs (168 genes; Fig. 5B; Supplementary Table 3). We individually confirmed their
335 gene annotations and associated GO terms. Clustering the resulting table by genes and GO
336 terms reveals two dominant signatures (Fig. 5B). Many GO terms are associated with circadian
337 timing and are driven by a small number of genes, which include almost all core circadian clock
338 genes (Fig. 5B and C). As a second strong signal, almost half of the genes are annotated with
339 biological processes involved in nervous system development (Fig. 5B and C). GO term enrich-
340 ment is also found for ecdysteroid metabolism, imaginal disc development and gonad devel-
341 opment (Fig. 5). These processes of pre-pupal development are expected to be under circal-
342 unar clock control. The fact that circalunar clocks are responsive to moonlight and water tur-
343 bulence[9] renders the finding of GO term enrichment for "auditory behaviour" and "photo-
344 taxis" interesting. Furthermore, many of the genes involved in nervous system development
345 and sodium ion transport, also have GO terms that implicate them in light- and mechanore-
346 ceptor development, wiring or sensitivity (Supplementary Data 5). With the exception of "re-
347 sponse to hypoxia" and possibly "sodium ion transmembrane transport", there are very few
348 GO terms that can be linked to the submerged larval habitat of the *Baltic ecotype*, which is
349 usually low in salinity and can turn hypoxic in summer. There is a striking absence of GO terms
350 involved in metabolic processes or immune response.
351 Taken together, the detected GO terms are highly consistent with the known ecotype dif-
352 ferences and suggest that ecotypes are mainly defined by changes in the circadian clock and
353 nervous system development. A previously unknown aspect of *Clunio* ecotype formation is
354 highlighted by the GO terms "male courtship behaviour", "inter-male aggression" and "copu-
355 lation" (Fig. 5). These processes are subject to sexual selection and considered to evolve fast.
356 They could in the long term entail assortative mating between ecotypes.

357

358 **Strongly differentiated loci correspond to GO-term enriched biological processes.** While
359 GO term analysis gives a broad picture of which processes have many genes affected by eco-
360 type-associated SNPs, this does not necessarily imply that these genes and processes also
361 show the strongest association with ecotype. Additionally, major genes might be missed be-
362 cause they were not assigned GO terms. As a second line of evidence, we therefore selected
363 variants with the highest ecotype-association by increasing the eBP_{mc} cut-off to 10. This re-
364 duced the set of affected genes from 1,400 to 69 (Supplementary Data 6 and 7). Additionally,
365 we only considered genes with variants that are strongly differentiated between the ecotypes
366 ($F_{ST} \geq 0.75$, compare Fig. 3E), leaving thirteen genes in eight distinct genomic regions (Fig. 6A;
367 numbered in Fig. 3E). Two of these regions contain two genes each with no homology outside
368 *C. marinus* (indicated by "NA", Fig. 6A), confirming that GO term analysis missed major loci
369 because of a lack of annotation. Three other regions contain the – likely non-visual – photore-
370 ceptor *ciliary Opsin 1* (*cOps1*)[29], the transcription factor *longitudinals lacking* (*lola;* in fruit fly
371 involved in axon guidance[30] and photoreceptor determination[31]) and the nuclear receptor *tail-*
372 *less* (*tll;* in fruit fly involved in development of brain and eye[32]), underscoring that ecotype
373 characteristics might involve differential light sensitivity. Interestingly, *tll* also affects develop-
374 ment of the neuroendocrine centres involved in ecdysteroid production and adult emer-
375 gence[33]. Even more, re-annotation of this genomic locus revealed that the neighbouring gene,
376 which is also affected by ecotype specific variants, is the *short neuropeptide F receptor* (*sNPF-*
377 *R*) gene. Among other functions, sNPF-R is involved in coupling adult emergence to the circa-
378 dian clock[34]. Similarly, only 100 kb from *cOps1* there is the differentiated locus of *matrix met-*
379 *alloprotease 1* (*Mmp1*), which is known to regulate circadian clock outputs via processing of
380 the neuropeptide *pigment dispersing factor* (PDF)[35]. In both cases, the close genetic linkage
381 could possibly form pre-adapted haplotypes and entail a concerted alteration of sensory and
382 circadian functions in the formation of ecotypes. In the remaining two loci, *sox100B* is known
383 to affect male gonad development[36] and the *ecdysone-induced protein 93F* is involved in re-
384 sponse to hypoxia in flies[37], but was recently found to also affect reproductive cycles in mos-
385 quitoes[38]. In summary, only two out of the top 13 ecotype-associated genes were comprised

386 in the top 40 GO terms (Fig. 6A). Nevertheless, all major biological processes detected in GO
387 term analysis (Fig. 5) are also reflected in the strongly ecotype-associated loci (Fig. 6), giving a
388 robust signal that circadian timing, sensory perception and nervous system development are
389 underlying ecotype formation in *C. marinus*.

390 Finally, we assessed the top 13 strongly ecotype-associated loci for signatures of selective
391 sweeps in genetic diversity and LD (Fig. 6B-G). Despite these loci being the most differentiated
392 between ecotypes in the entire genome, there is at best a mild reduction in genetic diversity
393 and a mild increase in LD (Fig. 6B-G). If selection acted on these loci, it must have been very
394 soft, underscoring a history of polygenic adaptation from standing genetic variation and con-
395 tinued recombination.

A

Locus	Chromosome	Scaffold	Start position	CLUMA CG number	Gene	SNPs: CDS: non-synonymous	SNPs: CDS: synonymous	SNPs: Stop retained	SNPs: Splice site	SNPs: 3' UTR	SNPs: 5' UTR	SNPs: Intron	SNPs: Intergenic	Indels: Inframe (conservative)	Indels: 3' UTR	Indels: Intron	Indels: Intergenic	detected via GO term
①	1	6	68627	020452	Novel nucleolar protein 2 (Non2)	.	.	.	.	.	.	.	20	.	.	.	3	
	1	6	88768	020457	Ecdysone-induced protein 93F (Eip93F)	.	.	.	.	.	.	9	20	.	.	2	3	Y
②	1	18	629474	002631	pupal cuticle protein 78E (pcp78E)	.	.	.	.	.	.	.	22	.	.	.	6	
	1	18	649185	002673	tailless (tll)	1	.	.	.	.	.	.	36	.	.	.	11	Y
	1	18	669600	002806	*is part of* sNPF receptor (sNPF-R; CG002648)	.	.	.	.	.	.	.	15	.	.	.	5	
③	1	18	1240686	002670	NA	4	1	1	1	.	.	4	7	1	.	2	.	
	1	18	1243996	002667	NA	1	2	.	.	2	.	.	13	.	.	.	5	
④	1	18	1282649	002573	longitudinals lacking (lola)	.	.	.	.	.	.	24	1	.	1	15	.	
⑤	1	43	1081770	008519	Matrix metalloproteinase 1 (Mmp1)	.	.	.	1	24	.	52	.	.	2	6	.	
⑥	1	43	985815	008485	ciliary Opsin 1 (cOps1)	2	2	.	.	.	.	8	37	.	.	5	10	
⑦	1	43	511465	008347	NA	.	.	.	.	.	.	.	33	.	.	.	6	
	1	43	523131	023379	NA	7	2	.	.	.	.	.	22	.	.	.	6	
⑧	1	42	676396	008160	SOX-100B	.	.	.	.	.	.	5	.	.	.	2	.	

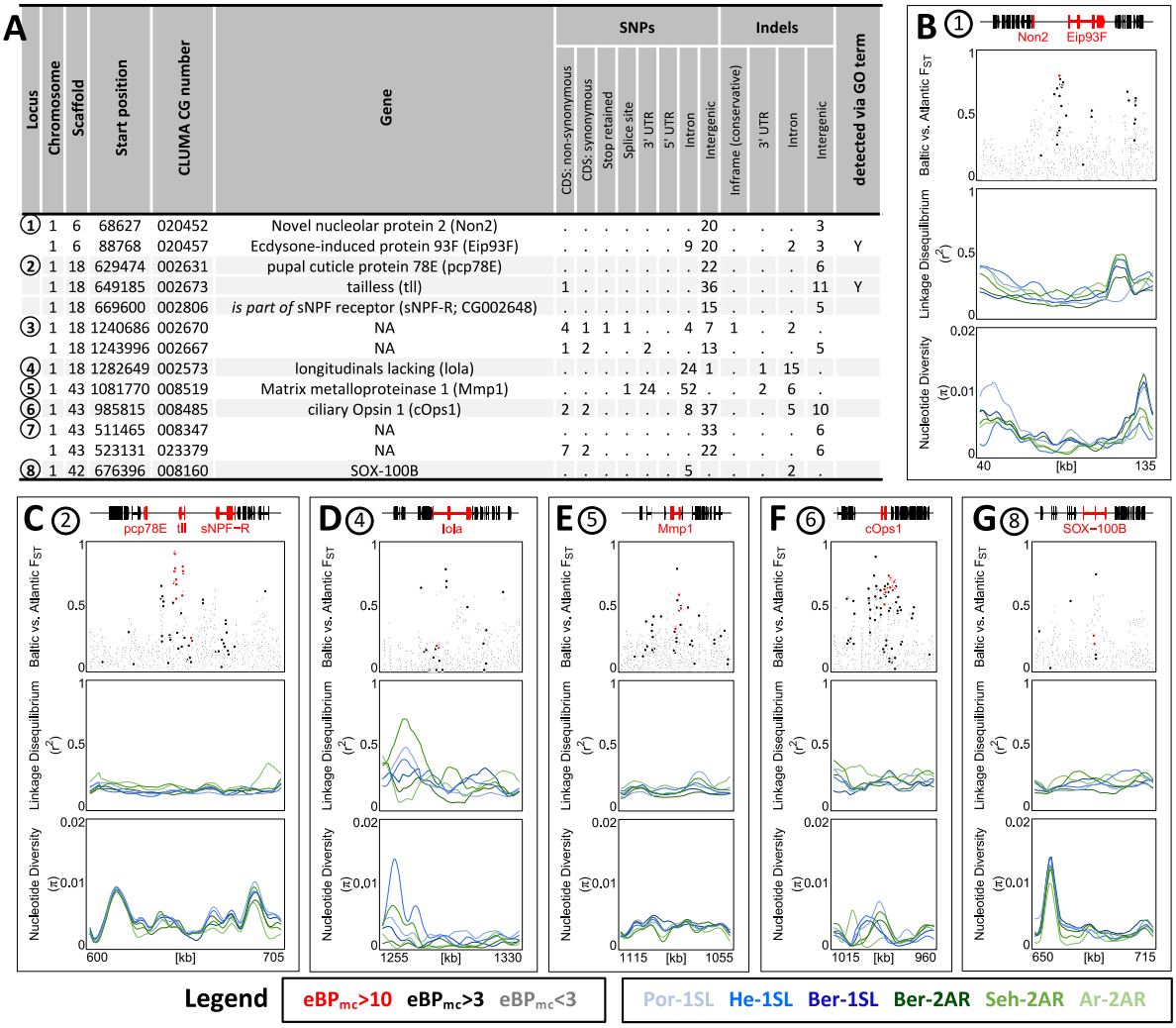

Figure 6 **The 13 most differentiated ecotype-associated genes**

(**A**) Loci with highly ecotype-associated variants were selected based on eBPmc > 3 and F_{ST}(Baltic-Atlantic) > 0.75. There are 13 genes in eight distinct genomic loci. (**B-G**) An overview is given for the six loci with identified genes. In each panel, from top to bottom the sub-panels show the gene models, F_{ST} values of genetic variants in the region, local linkage disequilibrium (LD) and genetic diversity (π). F_{ST} values are coloured by ecotype association of the variant (red: eBP_{mc} > 10; black: 10 > eBP_{mc} > 3; grey: eBP_{mc} < 3). LD and genetic diversity are shown for the six populations independently, coloured-coded as in Fig. 1 and 2. The are no strong signatures of selection.

407 ## Discussion

408 The deep genomic analysis of *Clunio* populations has allowed to reconstruct a detailed bi-
409 ogeographic history of their different ecotypes. Most surprisingly, the two sympatric ecotypes
410 that were considered different species turned out to be the most closely related populations
411 in the sample, testifying the high power of ecology in generating differential adaptation in the
412 face of gene flow. The data allowed further to infer a polygenic architecture for ecotype for-
413 mation. We found that while ecotype-associated alleles differ in allele frequency, they are
414 largely shared between ecotypes, which suggests that adaptation primarily involves standing
415 genetic variation from many different loci. A similar re-use of existing regulatory variation has
416 been found in ecotype formation in sticklebacks[39-41] or mimicry in *Heliconius* butterflies[42].
417 However, while in *Heliconius* alleles are shared over large evolutionary distances via introgres-
418 sion, *Clunio* ecotypes diverged recently from a common source, as is illustrated by massive
419 and genome-wide shared polymorphism. Combined with the observation that many genes
420 from the same biological processes have ecotype-associated alleles, this draws a picture of
421 polygenic adaptation, involving many pre-existing alleles with probably small phenotypic ef-
422 fects. Particularly for adaptation in circadian timing this scenario is highly plausible. The an-
423 cestral *Atlantic ecotype* comprises many genetically determined circadian timing types that
424 are adapted to the local tides[11,12,14,43]. Existing genetic variants conveying emergence at dusk
425 were likely selected or re-assorted to form the *Baltic ecotype*'s highly concentrated emer-
426 gence at dusk.

427 Besides circadian timing, the ecotypes differ in circalunar timing and oviposition behavior.
428 In our study the vast majority of GO terms and candidate genes is consistent with these func-
429 tions, leaving little risk for evolutionary "story-telling" based on individual genes or GO
430 terms[44]. We propose that good congruence between known phenotypic differences and de-
431 tected biological processes could be a hallmark of polygenic adaptation, as only polygenic ad-
432 aptation is expected to leave a footprint in many genes of the same ecologically relevant bio-
433 logical process.

434 Based on our genomic comparison of lunar-rhythmic and lunar-arrhythmic ecotypes, we
435 propose three not mutually exclusive hypotheses on molecular pathways involved in the

436 unknown circalunar clock. Firstly, *Clunio*'s circalunar clock is known to tightly regulate ecdys-
437 teroid-dependent development and maturation just prior to pupation[45]. Congruently, our
438 screen identified ecotype-associated genes in the development of imaginal discs and genital
439 discs, and in ecdysteroid metabolism. Lunar arrhythmicity may rely on an escape of these pro-
440 cesses from circalunar clock control. Secondly, it has been hypothesized that circalunar clocks
441 involve a circadian clock[46] and such a mechanism has been experimentally confirmed in the
442 midge *Pontomyia oceana*[47]. Thus, the overwhelming circadian signal in our data might be re-
443 sponsible for both circadian timing adaptations and the loss of circalunar rhythms. Thirdly,
444 *Clunio*'s circalunar clock is synchronized with the external lunar cycle via moonlight, as well as
445 tidal cycles of water turbulence and temperature[9]. Our data suggests that sensory receptor
446 development, wiring or sensitivity might differ between ecotypes. Interestingly, some *Atlantic*
447 *ecotype* populations are insensitive to specific lunar time cues, either moonlight or mechanical
448 stimulation by the tides[11]. These pre-existing insensitivities may have been combined to form
449 completely insensitive and hence lunar-arrhythmic ecotypes. This scenario would fit the gen-
450 eral pattern of polygenic adaptation through a re-assortment of standing genetic variation,
451 which emerges from our study.

452 In several species, genes involved in complex behavioral or ecological syndromes were
453 found to be locked into supergenes by chromosomal inversions, e.g. in *Heliconius* butterfly
454 mimicry[48] or reproductive morphs of the ruff[49]. While we observe a clustering of ecotype-
455 associated alleles in *Clunio*, there is no obvious connection to an underlying structural variant
456 (SV). Possibly, the SV is so complex that it did not leave an interpretable genomic signal. Alter-
457 natively, *Clunio*'s long history of genome rearrangements[14] may have resulted in a clustering
458 of ecologically relevant loci without locking them into a single SV. Clustering could be stabi-
459 lized by low recombination, consistent with the observed three LD blocks, which – while not
460 ecotype-specific – all overlap with the differentiated region. Epistatic interactions between
461 the clustered loci and co-adaptation of alleles might further reduce the fitness of recombi-
462 nants and lead to a concerted response to selection. Such an interconnected adaptive cluster
463 might allow for more flexible evolutionary responses than a single, completely linked

464 supergene. Further studies will have to show whether such a genome architecture exists,
465 whether it facilitates adaptation and whether it might itself be selected for.

466 # Methods

467

468 **Nomenclature of ecotypes.** We expanded the existing naming convention of *C. marinus*
469 timing types[43] to also include *Baltic* and *Arctic ecotypes*. Names of populations and corre-
470 sponding laboratory strains consist of an abbreviation for geographic origin followed by a code
471 for the daily and lunar timing phenotypes. Daily phenotypes in this study are emergence dur-
472 ing the first 12 hours after sunrise ("1") or, emergence during the second 12 hours after sun-
473 rise ("2") or emergence during every low tide ("t" for tidal rhythm). Lunar phenotypes in this
474 study are either emergence during full moon and new moon low tides ("SL" for semi-lunar) or
475 arrhythmic emergence ("AR"). As a consequence, the *Arctic ecotype* is "tAR", the *Baltic eco-*
476 *type* is "2AR" and the *Atlantic ecotype* populations in this study are all of timing type "1SL"
477 (while other timing types exist within the *Atlantic ecotype*[43]).

478

479 **Fieldwork and sample collection.** Field samples for genetic analysis and establishment of
480 laboratory strains were collected in Sehlendorf (Seh, Germany), Ar (Sweden), Tromsø (Tro,
481 Norway) and Bergen (Ber, Norway) during eight field trips in 2017 and 2018 (Supplementary
482 Tab. 4). Field caught adult males for DNA extraction were directly collected in 99.98 % ethanol
483 and stored at -20°C. Females are immobile and basically invisible in the field, unless found in
484 copulation. Laboratory strains were established by catching copulating pairs in the field and
485 transferring multiple fertilized egg clutches to the laboratory (Supplementary Tab. 4). Samples
486 and laboratory strains of the sympatric ecotypes in Bergen were collected at the same location
487 but at different daytime. Additional samples and laboratory strains from Helgoland (He, Ger-
488 many) and Port-en-Bessin (Por, France) were collected and described earlier[14,43,50], but had
489 previously not been subject to whole genome sequencing of individuals.

490

491 **Laboratory culture and phenotyping of ecotypes.** Laboratory strains were reared under
492 standard conditions[51] at 20°C with 16 h of light and 8 h of darkness. *Atlantic* and *Arctic ecotype*
493 strains were kept in natural seawater diluted 1:1 with deionized water and fed with diatoms
494 (*Phaeodactylum tricornutum*) and powdered nettles (*Urtica sp.*). The *Baltic ecotype* was kept

495 in natural Sea water diluted 1:2 and fed with diatoms and powdered red algae (90%, *Delesseria*
496 *spp.*, 10% *Ceramium spp.*, obtained from F. Weinberger and N. Stärck, GEOMAR, Kiel). For
497 entrainment of the lunar rhythm all strains were provided with 12.4 h tidal cycles of water
498 turbulence (mechanically induced vibrations produced by an unbalanced motor, 50 Hz,
499 roughly 30 dB above background noise, 6.2 h on, 6.2 h off)[52,53].

500 Assignment of strains to ecotypes was confirmed based on their phenotypes as recorded
501 in laboratory culture. Oviposition behavior was assessed during standard culture mainte-
502 nance: *Baltic ecotype* eggs are generally found submerged at the bottom of the culture vessel,
503 *Atlantic* and *Arctic ecotype* eggs are always found floating on the water surface or on the walls
504 of the culture vessel (see Supplementary Note 1). Daily emergence times were recorded in 1h
505 intervals by direct observation (Seh-2AR, Ar-2AR) or with the help of a fraction collector[54] (Ber-
506 1SL, Ber-2AR, Tro-tAR, Por-1SL, He-1SL; Supplementary Fig. 1). Lunar emergence times were
507 recorded by counting the number of emerged midges in the laboratory cultures every day
508 over several months and summing them up over several tidal turbulence cycles. Emergence
509 data for He-1SL was taken from[55], emergence data for Por-1SL was taken from a manuscript
510 in preparation (D Briševac, C Prakash, TS Kaiser).

511

512 **Crosses and Quantitative Trait Locus (QTL) mapping.** The Ber-1SL and Ber-2AR laboratory
513 strains were subject to single-pair crossing after their emergence rhythms were synchronized
514 by keeping them in separate, time-shifted LD regimes. Several F1 families were raised inde-
515 pendently and the F1 siblings were allowed to mate freely in order to obtain bulk F2 families.
516 Emergence distributions were recorded by collecting all emerged adults every day.

517 Bulk crossing family 34 (n=272) was selected for QTL mapping. DNA of the two parents and
518 the F2 progeny was extracted with the QuickExtract DNA Extraction Solution (Lucigen,
519 QE0905T) according to manufacturer's protocol with modifications. Instead of vortexing be-
520 fore incubation, a pestle was used to grind the sample. In order to identify scorable markers
521 for the genetically very similar strains, the two parents of the cross were subject to whole-
522 genome sequencing. Raw reads were processed through our genotyping pipeline (described
523 below), resulting in 656,368 detected variants, 53,097 of which were diagnostic for the

524 grandparents. Based on the list of diagnostic markers, we picked eight evenly spaced regions
525 on each chromosome for amplicon sequencing (Supplementary Fig. 21, Supplementary Tab.
526 5). Multiplex PCR was performed with the QIAGEN Multiplex PCR Kit (206143) for each chro-
527 mosome primer set separately (15 min at 95°C; 40 cycles of 94°C for 30 s, 57°C for 90 s and
528 72°C for 90 s; 72°C for 10 min). Sequencing libraries were prepared with standard Illumina
529 protocols and sequenced with 150 bp paired-end on the Illumina HiSeq3000 sequencer by the
530 Max Planck Genome Centre (Cologne, Germany). Sequencing reads from independent runs
531 were first merged to one read file for forward and reverse reads. Those files were again sub-
532 ject to our genotyping pipeline (described below) with the exception that the mapped reads
533 in SAM format undergone a coverage capping of 40 using a custom python script and the VCF
534 was filtered for a minimum minor allele frequency of 0.25 ('--maf 0.25') and a maximum pro-
535 portion of missing data per locus of 30% ('--max-missing 0.7'). All markers that were not diag-
536 nostic for the parents were removed. In case genotypes differed within an amplicon, a con-
537 sensus amplicon genotype was called by majority.
538 For QTL mapping the degree of rhythmicity of an individual was recorded as the number of
539 days between its emergence day and day 9, which is the peak of emergence in the rhythmic
540 strain (Ber-1SL). As this phenotype is not normally distributed (Kolmogorov-Smirnov test and
541 the Shapiro-Wilk test of normality) it was treated as non-parametric. QTL scans were per-
542 formed in the R package 'qtl' [56]. The genome scans with different QTL models followed the
543 calculation of conditional genotype probabilities in 5 cM distances and simulated genotypes
544 from 64 imputations with the same distance. Both phenotypes (lunar rhythmicity, sex) were
545 scanned for a single QTL model in the 'scanone()' function (method = "em"). Significance
546 thresholds were set at top 5% of the logarithm of the odds (LOD) scores for 1000 permuta-
547 tions. The 'stepwise.qtl()' function for identification of multiple and interacting QTLs returned
548 a null QTL model for lunar rhythmicity.
549
550 **DNA extraction and whole genome sequencing.** For each of the seven populations, 24 field
551 caught males (23 for Por-1SL, 25 for He-1SL) were subject to whole genome sequencing. DNA
552 was extracted from entire individuals with a salting out method[57] and amplified using the

553 REPLI-g Mini Kit (QIAGEN) according to the manufacturer's protocol with volume modifica-
554 tions (Supplementary Tab. 6). All samples were subject to whole genome shotgun sequencing
555 at 15-20x target coverage on an Illumina HiSeq3000 sequencer with 150 bp paired-end reads.
556 Library preparation and sequencing were performed by the Max Planck Genome Centre (Co-
557 logne, Germany) according to standard protocols. Raw sequence reads are deposited at ENA
558 under Accession PRJEB43766.
559
560 **Sequence data processing, genotyping and SNP filtering.** Raw sequence reads were
561 trimmed for adapters and base quality using Trimmomatic v.0.38[58] with parameters 'ILLUMI-
562 NACLIP:TruSeq3-PE-2.fa:2:30:10:8:true', 'LEADING:20', 'TRAILING:20', 'MINLEN:75'. Overlap-
563 ping paired end reads were merged with PEAR v.0.9.10[59], setting the minimum assembled
564 sequence length to 75 bp and a capping quality score of 20. Assembled and unassembled
565 reads were mapped with BWA-MEM[60] to the nuclear reference genome[14] (ENA accession
566 GCA_900005825.1) and the mitochondrial reference genome (ENA accession
567 CVRI01023763.1) of *C. marinus*. Mapped reads were sorted, indexed, filtered for mapping
568 quality (-q 20) and transformed to BAM format with SAMtools v.1.9[61]. Read group information
569 was added with the AddOrReplaceReadGroups.jar v.1.74 script from the Picard toolkit
570 (http://picard.sourceforge.net/) [62].
571 For the nuclear genome, SNPs and insertion-deletion (indel) genotypes were called using
572 GATK v.3.8-0-ge9d806836[63]. After initial genotype calling with the GATK HaplotypeCaller and
573 the parameter '-stand_call_conf 30', base qualities were recalibrated with the GATK Bas-
574 eRecalibrator with '-knownSites' and genotype calling was repeated on the recalibrated BAM
575 files to obtain the final individual VCF files. Individual VCF files were combined using GATK
576 GenotypeGVCFs. SNP and indel genotypes were filtered with VCFtools v.0.1.14 [64] to keep only
577 biallelic polymorphisms (--max-alleles 2), with a minimum minor allele frequency of 0.02 (--
578 maf 0.02), a minimum genotype quality of 20 (--minQ 20) and a maximum proportion of miss-
579 ing data per locus of 40% (--max-missing 0.6), resulting in 792,032 SNPs and 156,096 indels
580 over the entire set of 168 individuals. For certain analyses indels were excluded with VCFtools
581 ('--remove-indels').

582 Reads mapped to the mitochondrial genome were transformed into mitochondrial haplo-
583 types as described in [65].
584
585 **Population genomic analyses.** Mitochondrial haplotype networks were calculated using
586 the Median-Joining algorithm[66] with Network v.10.1.0.0 (fluxus-engineering.com).
587 Nuclear SNP genotypes were converted to PLINK format with VCFtools. SNPs were LD
588 pruned with PLINK v.1.90b4[67] and parameters '--indep-pairwise 50 10 0.5' as well as '--chr-set
589 3 no-xy no-mt --nonfounders'. Principal Component Analysis (PCA) was performed in PLINK
590 using the option '--pca' with the options default settings. The pruned BED file from PLINK was
591 used as input to ADMIXTURE v.1.3.0[68], with which we assessed a series of models for K=1 to
592 K=10 genetic components, as well as the corresponding the cross-validation error ('--cv'). Mi-
593 gration was further tested by converting the SNP data to TreeMix format with the *vcf2tree-*
594 *mix.sh* script[69] and running *TreeMix 1.13*[70] with default parameters and the southernmost Por-
595 1SL as root population.
596 Population estimates along the chromosomes were calculated in 100 kb overlapping slid-
597 ing-windows with 10 kb steps. Nucleotide diversity (π) was calculated for SNPs with VCFtools
598 '--window-pi'. For the genome-wide average, calculations were repeated with 200kb non-
599 overlapping windows. Linkage disequilibrium (LD; as r^2) was calculated in VCFtools with '--
600 geno-r2'. Local LD was calculated with '--ld-window-bp 500'. Preliminary tests showed that
601 local LD decays within a few hundred base pairs (Supplementary Fig. 22). For long range LD
602 minor allele frequency was filtered to 0.2 ('--maf 0.2', resulting in 335,800 SNPs), only values
603 larger 0.5 were allowed with '--min-r2 0.5' and the '--ld-window-bp 500' filter was removed.
604 Pairwise F_{ST} was calculated with VCFtools '--weir-fst-pop' option per SNP and in sliding win-
605 dows. For calculation of genetic divergence (d_{xy}), allele frequencies were extracted with
606 VCFtools '--freq' and d_{xy} was estimated from allele frequencies according to [71].
607
608 **Phylogenomics and topology weighting.** Nuclear genome phylogeny was calculated for a
609 random set of six individuals from each population, without Tro-tAR (n=36). For windowed
610 phylogenies, the VCF file was subset into non-overlapping 50 kb windows using VCFtools '--

611 from-bp --to-bp'. SNP genotypes were transformed into FASTA alignments of only informative
612 sites with the vcf2phylip.py v.2.3 script[72] and parameters '-m 1 -p -f'. Heterozygous genotypes
613 were represented by the respective IUPAC code for both bases. Whole genome and windowed
614 phylogenies were calculated with IQ-TREE v.1.6.12 [73] using the parameters '-st DNA -m MFP -
615 keep-ident -redo' for the windowed and '-st DNA -m MFP -keep-ident -bb 1000 -bnni -nt 10 -
616 redo' for the whole genome phylogenies. Topology weighting was performed on the win-
617 dowed phylogenies with TWISST [74] and the parameter '--method complete'.
618
619 **Association analysis.** Population-based association between genetic variants (SNPs and In-
620 dels) and ecotype, as well as environmental variables (Supplementary Tab. 7) was assessed in
621 BayPass v.2.2 [27]. Allele counts were obtained with VCFtools option '--counts'. Analyzed covari-
622 ates were ecotype, sea surface salinity (obtained from [75]) and average water temperature of
623 the year 2020 (obtained from weather-atlas.com, accessed 27.04.2020; 16:38), as given in
624 Supplementary Tab. 7. BayPass was run with the MCMC covariate model. BayPass corrects for
625 population structure via Ω dissimilarity matrices, then calculates the X^tX statistics and finally
626 assesses the approximate Bayesian p value of association (eBP_{mc}). To obtain a significance
627 threshold for X^tX values, the data was randomly subsampled (100,000 genetic variants) and
628 re-analyzed with the standard covariate model, as implemented in baypass_utils.R. All ana-
629 lyses we performed in three replicates (starting seeds 5001, 24306 and 1855) and the median
630 is shown.
631
632 **SNP effects and GO term enrichment analysis.** Gene annotations to the CLUMA1.0 refer-
633 ence genome [14] were considered reliable if they fulfilled one of three criteria: 1) Identified
634 ortholog in UniProtKB/Swiss-Prot or non-redundant protein sequences (nr) at NCBI or PFAM
635 domain, as reported in [14]. 2) Overlap of either at least 20% with mapped transcript data or
636 40% with mapped protein data, as reported in [14]. 3) Manually annotated. This resulted in a
637 15,193 confidence genes models. The location and putative effects of the SNPs and indels
638 relative to these confidence gene models were annotated using SnpEff 4.5 [28] (build 2020-04-
639 15 22:26, non-default parameter `-ud 0'). Gene Ontology (GO) terms were annotated with

640 emapper-2.0.1. [76] from the eggNOG 5.0 database[77], using DIAMOND [78], BLASTP e-value <$1e^{-10}$
641 and subject-query alignment coverage of >60%. Conservatively, we only transferred GO terms
642 with "non-electronic" GO evidence from best-hit orthologs restricted to an automatically ad-
643 justed per-query taxonomic scope, resulting in 5,393 *C. marinus* gene models with GO term
644 annotations. Enrichment of "Biological Process" GO terms in the genes associated with eco-
645 type-specific polymorphisms was assessed with the weight01 Fisher's exact test implemented
646 in topGO [79] (version 2.42.0, R version 4.0.3).
647
648 **Figure preparation.** Figures were prepared in R[80]. Data were handled with the 'data.table'[81]
649 and 'plyr'[82] packages. The map of Europe was generated using the packages 'ggplot2'[83] and
650 'ggrepel' [84], 'maps'[85] and 'mapdata'[86]. The map was taken from the CIA World DataBank II
651 (http://www.evl.uic.edu/pape/data/WDB/). Circular plots were prepared using the R package
652 'circlize'[87]. Multiple plots were combined in R using the package 'Rmisc'[88]. The graphical edit-
653 ing of the whole genome phylogeny was done in Archeopteryx (http://www.phylosoft.org/ar-
654 chaeopteryx)[89]. Final figure combination and graphical editing of the raw plot files was done
655 in *Inkscape*. Neighbor Joining trees of the omega statistic distances from BayPass were created
656 with the R package 'ape'.[90] In all plots the order and orientation of scaffolds within the chro-
657 mosomes follows the published genetic linkage map[14].

Data availability

Sequencing data for field samples and mapping families are deposited at ENA under Accession PRJEB43766. Filtered genome annotations are given in Supplementary Dataset 2.

Acknowledgements

For field work we obtained logistic support from the Ar Research Station (Uppsala University), the Marine Biological Station Espegrend (University of Bergen), Even Jørgensen (The Arctic University of Norway, Tromsø) and Florian Weinberger and Nadja Stärck (GEOMAR Helmholtz Centre for Ocean Research Kiel). We thank Jürgen Reunert, Kerstin Schäfer and Susanne Mentz for technical assistance, as well as all members of the MPRG "Biological Clocks" for discussion and support. Diethard Tautz and Julien Dutheil critically read the manuscript. Whole genome sequencing was performed at the Max Planck Genome Center (Cologne) with financial support from the Max Planck Society. This work was funded by the Max Planck Society through the Max Planck Research Group "Biological Clocks" and a sequencing grant. The work was further funded by the European Research Council (ERC) under the Horizon 2020 research and innovation program with an ERC Starting Grant (Grant agreement 802923) awarded to TSK.

Author contributions

NF performed field work, laboratory work, QTL mapping, population genomic analyses and association analysis, prepared the figures and participated in drafting the manuscript. CP analyzed SNP effects and GO term enrichment and participated in figure preparation. TSK conceived, designed and supervised the study, participated in data analysis and figure preparation and wrote the manuscript. All authors approved of the final manuscript.

Competing interests

There are no competing interests.

References

1 Wu, C.-I. & Ting, C.-T. Genes and speciation. *Nature Reviews Genetics* **5**, 114-122 (2004).

2 Phadnis, N. & Orr, H. A. A single gene causes both male sterility and segregation distortion in Drosophila hybrids. *science* **323**, 376-379 (2009).

3 Nosil, P. & Schluter, D. The genes underlying the process of speciation. *Trends in ecology & evolution* **26**, 160-167 (2011).

4 Hof, A. E. *et al.* The industrial melanism mutation in British peppered moths is a transposable element. *Nature* **534**, 102-105 (2016).

5 Sella, G. & Barton, N. H. Thinking about the evolution of complex traits in the era of genome-wide association studies. *Annual review of genomics and human genetics* **20** (2019).

6 Boyle, E. A., Li, Y. I. & Pritchard, J. K. An expanded view of complex traits: from polygenic to omnigenic. *Cell* **169**, 1177-1186 (2017).

7 Barton, N. H. The "New Synthesis". *Proceedings of the National Academy of Sciences* **119**, e2122147119, doi:doi:10.1073/pnas.2122147119 (2022).

8 Barghi, N., Hermisson, J. & Schlötterer, C. Polygenic adaptation: a unifying framework to understand positive selection. *Nature Reviews Genetics* **21**, 769-781 (2020).

9 Neumann, D. in *Annual, Lunar, and Tidal Clocks* (eds Hideharu Numata & Barbara Helm) Ch. 1, 3-24 (Springer Japan, 2014).

10 Andreatta, G. & Tessmar-Raible, K. The still dark side of the moon: molecular mechanisms of lunar-controlled rhythms and clocks. *J Mol Biol* **432**, 3525-3546 (2020).

11 Kaiser, T. S. in *Annual, Lunar, and Tidal Clocks* (eds Hideharu Numata & Barbara Helm) Ch. 7, 121-141 (Springer Japan, 2014).

12 Neumann, D. Genetic adaptation in emergence time of *Clunio* populations to different tidal conditions. *Helgoländer wissenschaftliche Meeresuntersuchungen* **15**, 163-171 (1967).

13 Kaiser, T. S., Neumann, D. & Heckel, D. G. Timing the tides: Genetic control of diurnal and lunar emergence times is correlated in the marine midge *Clunio marinus*. *BMC Genetics* **12**, 49, doi:10.1186/1471-2156-12-49 (2011).

14 Kaiser, T. S. *et al.* The genomic basis of circadian and circalunar timing adaptations in a midge. *Nature* **540**, 69-73, doi:10.1038/nature20151 (2016).

15 Kaiser, T. S. & Heckel, D. G. Genetic Architecture of Local Adaptation in Lunar and Diurnal Emergence Times of the Marine Midge *Clunio marinus* (Chironomidae, Diptera). *PLoS ONE* **7**, e32092, doi:10.1371/journal.pone.0032092 (2012).

16 Remmert, H. Ökologische Untersuchungen über die Dipteren der Nord- und Ostsee. *Archiv für Hydrobiologie* **51**, 1-53 (1955).

17 Endraß, U. Physiologische Anpassungen eines marinen Insekts. I. Die zeitliche Steuerung der Entwicklung. *Marine Biology* **34**, 361-368 (1976).

18 Palmén, E. & Lindeberg, B. The marine midge, Clunio marinus Hal. (Dipt., Chironomidae), found in brackish water in the northern Baltic. *Internationale Revue der gesamten Hydrobiologie und Hydrogeographie* **44**, 383-393 (1959).

19 Neumann, D. & Honegger, H. W. Adaptations of the Intertidal Midge Clunio to Arctic Conditions. *Oecologia* **3**, 1-13 (1969).

20 Pflüger, W. & Neumann, D. Die Steuerung einer gezeitenparallelen Schlüpfrhythmik nach dem Sanduhr-Prinzip. *Oecologia* **7**, 262-266 (1971).

21 Endraß, U. Physiologische Anpassungen eines marinen Insekts. II. Die Eigenschaften von schwimmenden und absinkenden Eigelegen. *Marine Biology* **36**, 47-60 (1976).

22 Heimbach, F. Sympatric species, Clunio marinus Hal. and Cl. balticus n. sp. (Dipt., Chironomidae), isolated by differences in diel emergence time. *Oecologia* **32**, 195-202 (1978).

23 Patton, H. *et al.* Deglaciation of the Eurasian ice sheet complex. *Quaternary Science Reviews* **169**, 148-172 (2017).

24 Hofmann, W. & Winn, K. The littorina transgression in the Western Baltic Sea as indicated by subfossil Chironomidae (Diptera) and Cladocera (Crustacea). *International Review of Hydrobiology* **85**, 267-291 (2000).

25 Edelman, N. B. & Mallet, J. Prevalence and adaptive impact of introgression. *Annual Review of Genetics* **55**, 265-283 (2021).

26 Baack, E. J. & Rieseberg, L. H. A genomic view of introgression and hybrid speciation. *Current opinion in genetics & development* **17**, 513-518 (2007).

27 Gautier, M. Genome-wide scan for adaptive divergence and association with population-specific covariates. *Genetics* **201**, 1555-1579 (2015).

28 Cingolani, P. *et al.* A program for annotating and predicting the effects of single nucleotide polymorphisms, SnpEff: SNPs in the genome of *Drosophila melanogaster* strain w^{1118}; *iso*-2; *iso*-3. *Fly* **6**, 80-92, doi:10.4161/fly.19695 (2012).

29 Velarde, R. A., Sauer, C. D., Walden, K. K. O., Fahrbach, S. E. & Robertson, H. M. Pteropsin: A vertebrate-like non-visual opsin expressed in the honey bee brain. *Insect Biochemistry and Molecular Biology* **35**, 1367-1377 (2005).

30 Crowner, D., Madden, K., Goeke, S. & Giniger, E. Lola regulates midline crossing of CNS axons in Drosophila. *Development* **129**, 1317-1325 (2002).

31 Zheng, L. & Carthew, R. W. Lola regulates cell fate by antagonizing Notch induction in the Drosophila eye. *Mechanisms of Development* **125**, 18-29 (2008).

32 Suzuki, T. & Saigo, K. Transcriptional regulation of atonal required for Drosophila larval eye development by concerted action of eyes absent, sine oculis and hedgehog signaling independent of fused kinase and cubitus interruptus. *Development* **127**, 1531-1540 (2000).

33 de Velasco, B. *et al.* Specification and development of the pars intercerebralis and pars lateralis, neuroendocrine command centers in the Drosophila brain. *Developmental Biology* **302**, 309-323 (2007).

34 Selcho, M. *et al.* Central and peripheral clocks are coupled by a neuropeptide pathway in Drosophila. *Nature Communications* **8**, 15563, doi:10.1038/ncomms15563 (2017).

35 Depetris-Chauvin, A. *et al.* Mmp1 Processing of the PDF Neuropeptide Regulates Circadian Structural Plasticity of Pacemaker Neurons. *PLOS Genetics* **10**, e1004700, doi:10.1371/journal.pgen.1004700 (2014).

36 Nanda, S. *et al.* Sox100B, a Drosophila group E Sox-domain gene, is required for somatic testis differentiation. *Sexual Development* **3**, 26-37 (2009).

37 Lee, S.-J., Feldman, R. & O'Farrell, P. H. An RNA interference screen identifies a novel regulator of target of rapamycin that mediates hypoxia suppression of translation in Drosophila S2 cells. *Molecular Biology of the Cell* **19**, 4051-4061 (2008).

38 Wang, X. *et al.* The ecdysone-induced protein 93 is a key factor regulating gonadotrophic cycles in the adult female mosquito Aedes aegypti. *Proceedings of the National Academy of Sciences* **118** (2021).

39 Chan, Y. F. *et al.* Adaptive evolution of pelvic reduction in sticklebacks by recurrent deletion of a Pitx1 enhancer. *Science* **327**, 302-305 (2010).

40 Kingman, G. A. R. *et al.* Predicting future from past: The genomic basis of recurrent and rapid stickleback evolution. *bioRxiv* (2020).
41 Verta, J.-P. & Jones, F. C. Predominance of cis-regulatory changes in parallel expression divergence of sticklebacks. *Elife* **8**, e43785 (2019).
42 Edelman, N. B. *et al.* Genomic architecture and introgression shape a butterfly radiation. *Science* **366**, 594-599, doi:10.1126/science.aaw2090 (2019).
43 Kaiser, T. S., von Haeseler, A., Tessmar-Raible, K. & Heckel, D. G. Timing strains of the marine insect Clunio marinus diverged and persist with gene flow. *Molecular Ecology* **30**, 1264-1280, doi:https://doi.org/10.1111/mec.15791 (2021).
44 Pavlidis, P., Jensen, J. D., Stephan, W. & Stamatakis, A. A Critical Assessment of Storytelling: Gene Ontology Categories and the Importance of Validating Genomic Scans. *Molecular Biology and Evolution* **29**, 3237-3248, doi:Doi 10.1093/Molbev/Mss136 (2012).
45 Neumann, D. & Spindler, K. D. Circasemilunar Control of Imaginal Disk Development in Clunio marinus - Temporal Switching Point, Temperature-Compensated Developmental Time and Ecdysteroid Profile. *Journal of Insect Physiology* **37**, 101-109 (1991).
46 Bünning, E. & Müller, D. Wie messen Organismen lunare Zyklen? *Zeitschrift für Naturforschung* **16**, 391-395 (1962).
47 Soong, K. & Chang, Y.-H. Counting Circadian Cycles to Determine the Period of a Circasemilunar Rhythm in a Marine Insect. *Chronobiology International* **29**, 1329-1335, doi:10.3109/07420528.2012.728548 (2012).
48 Joron, M. *et al.* Chromosomal rearrangements maintain a polymorphic supergene controlling butterfly mimicry. *Nature* **477**, 203-U102, doi:10.1038/nature10341 (2011).
49 Küpper, C. *et al.* A supergene determines highly divergent male reproductive morphs in the ruff. *Nature Genetics* **48**, 79-83 (2016).
50 Kaiser, T. S., Neumann, D., Heckel, D. G. & Berendonk, T. U. Strong genetic differentiation and postglacial origin of populations in the marine midge *Clunio marinus* (Chironomidae, Diptera). *Molecular Ecology* **19**, 2845-2857, doi:10.1111/j.1365-294X.2010.04706.x (2010).
51 Neumann, D. Die lunare und tägliche Schlüpfperiodik der Mücke *Clunio* - Steuerung und Abstimmung auf die Gezeitenperiodik. *Zeitschrift für Vergleichende Physiologie* **53**, 1-61 (1966).
52 Neumann, D. & Heimbach, F. in *Cyclic Phenomena in Marine Plants and Animals* (eds E. Naylor & R.G. Hartnoll) 423-433 (Pergamon Press, 1979).
53 Neumann, D. Entrainment of a Semilunar Rhythm by Simulated Tidal Cycles of Mechanical Disturbance. *Journal of Experimental Marine Biology and Ecology* **35**, 73-85 (1978).
54 Honegger, H. W. An automatic device for the investigation of the rhythmic emergence pattern of Clunio marinus. *International Journal of Chronobiology* **4**, 217-221 (1977).
55 Neumann, D. Die zeitliche Programmierung von Tieren auf periodische Umweltbedingungen. *Rheinisch-Westfälische Akademie der Wissenschaften, Natur-Ingenieur- und Wirtschaftswissenschaften, Vortraege*, 31-62 (1983).
56 Broman, K. W., Wu, H., Sen, Ś. & Churchill, G. A. R/qtl: QTL mapping in experimental crosses. *bioinformatics* **19**, 889-890 (2003).
57 Reineke, A., Karlovsky, P. & Zebitz, C. P. W. Preparation and purification of DNA from insects for AFLP analysis. *Insect Molecular Biology* **7**, 95-99 (1998).

58 Bolger, A. M., Lohse, M. & Usadel, B. Trimmomatic: a flexible trimmer for Illumina sequence data. *Bioinformatics* **30**, 2114-2120 (2014).
59 Zhang, J., Kobert, K., Flouri, T. & Stamatakis, A. PEAR: a fast and accurate Illumina Paired-End reAd mergeR. *Bioinformatics* **30**, 614-620 (2014).
60 Li, H. Aligning sequence reads, clone sequences and assembly contigs with BWA-MEM. *arXiv preprint arXiv:1303.3997* (2013).
61 Li, H. *et al.* The Sequence Alignment/Map format and SAMtools. *Bioinformatics* **25**, 2078-2079, doi:10.1093/bioinformatics/btp352 (2009).
62 DePristo, M. A. *et al.* A framework for variation discovery and genotyping using next-generation DNA sequencing data. *Nature genetics* **43**, 491 (2011).
63 McKenna, A. *et al.* The Genome Analysis Toolkit: A MapReduce framework for analyzing next-generation DNA sequencing data. *Genome Research* **20**, 1297-1303, doi:10.1101/gr.107524.110 (2010).
64 Danecek, P. *et al.* The variant call format and VCFtools. *Bioinformatics* **27**, 2156-2158 (2011).
65 Fuhrmann, N. & Kaiser, T. S. The importance of DNA barcode choice in biogeographic analyses—a case study on marine midges of the genus Clunio. *Genome*, 1-11 (2020).
66 Bandelt, H. J., Forster, P. & Rohl, A. Median-joining networks for inferring intraspecific phylogenies. *Molecular Biology and Evolution* **16**, 37-48 (1999).
67 Chang, C. C. *et al.* Second-generation PLINK: rising to the challenge of larger and richer datasets. *Gigascience* **4**, s13742-13015-10047-13748 (2015).
68 Alexander, D. H. & Lange, K. Enhancements to the ADMIXTURE algorithm for individual ancestry estimation. *BMC Bioinformatics* **12**, 246, doi:10.1186/1471-2105-12-246 (2011).
69 Ravinet, M. <https://github.com/speciationgenomics/scripts/blob/master/vcf2treemix.sh> (last accessed 16th April 2021).
70 Pickrell, J. & Pritchard, J. Inference of population splits and mixtures from genome-wide allele frequency data. *Nature Precedings*, 1-1 (2012).
71 Delmore, K. E. *et al.* Genomic analysis of a migratory divide reveals candidate genes for migration and implicates selective sweeps in generating islands of differentiation. *Molecular Ecology* **24**, 1873-1888 (2015).
72 Ortiz, E. vcf2phylip v2. 0: convert a VCF matrix into several matrix formats for phylogenetic analysis. *URL https://doi. org/10.5281/zenodo* **2540861** (2019).
73 Nguyen, L.-T., Schmidt, H. A., Von Haeseler, A. & Minh, B. Q. IQ-TREE: a fast and effective stochastic algorithm for estimating maximum-likelihood phylogenies. *Molecular Biology and Evolution* **32**, 268-274 (2015).
74 Martin, S. H. & Van Belleghem, S. M. Exploring evolutionary relationships across the genome using topology weighting. *Genetics* **206**, 429-438 (2017).
75 Hordoir, R. *et al.* Nemo-Nordic 1.0: a NEMO-based ocean model for the Baltic and North seas–research and operational applications. *Geoscientific Model Development* **12**, 363-386 (2019).
76 Huerta-Cepas, J. *et al.* Fast genome-wide functional annotation through orthology assignment by eggNOG-mapper. *Molecular Biology and Evolution* **34**, 2115-2122 (2017).
77 Huerta-Cepas, J. *et al.* eggNOG 5.0: a hierarchical, functionally and phylogenetically annotated orthology resource based on 5090 organisms and 2502 viruses. *Nucleic Acids Research* **47**, D309-D314 (2019).

78 Buchfink, B., Xie, C. & Huson, D. H. Fast and sensitive protein alignment using DIAMOND. *Nature Methods* **12**, 59-60 (2015).
79 Alexa, A. & Rahnenfuhrer, J. topGO: enrichment analysis for gene ontology. *R package version* **2**, 2010 (2010).
80 Crawley, M. J. *The R Book*. (John Wiley & Sons Ltd., 2007).
81 Dowle, M. *et al.* Package 'data.table' version 1.13.2. *Extension of 'data. frame* (2020).
82 Wickham, H. The split-apply-combine strategy for data analysis. *Journal of Statistical Software* **40**, 1-29 (2011).
83 Wickham, H. *ggplot2: elegant graphics for data analysis*. (springer, 2016).
84 Slowikowski, K. *et al.* Package ggrepel. *Automatically Position Non-Overlapping Text Labels with 'ggplot2* (2018).
85 Brownrigg, R., Minka, T. & Deckmyn, A. maps: Draw Geographical Maps. R package version 3.3.0. (2018).
86 Becker, R., Wilks, A. & Brownrigg, R. mapdata: Extra map databases. R package version 2.3.0. (2018).
87 Gu, Z., Gu, L., Eils, R., Schlesner, M. & Brors, B. circlize implements and enhances circular visualization in R. *Bioinformatics* **30**, 2811-2812 (2014).
88 Hope, R. M. 'Rmisc: Ryan miscellaneous'. R package version 1.5. 2 (2013).
89 Han, M. V. & Zmasek, C. M. phyloXML: XML for evolutionary biology and comparative genomics. *BMC bioinformatics* **10**, 1-6 (2009).
90 Paradis, E. & Schliep, K. ape 5.0: an environment for modern phylogenetics and evolutionary analyses in R. *Bioinformatics* **35**, 526-528 (2019).